DALTON
FULL PAPER

# Synthesis, structures and magnetochemistry of binuclear cobalt(II), nickel(II) and copper(II) complexes of 2,6-diformyl-4-methylphenol dioxime

**Daniel Black,[a] Alexander J. Blake,[a] Keith P. Dancey,[b] Andrew Harrison,[c] Mary McPartlin,[b] Simon Parsons,[c] Peter A. Tasker,*[c,d] Gavin Whittaker[c] and Martin Schröder*[a]**

[a] *School of Chemistry, The University of Nottingham, University Park, Nottingham, UK NG7 2RD*
[b] *School of Chemistry, University of North London, London, UK N7 8DB*
[c] *Department of Chemistry, The University of Edinburgh, West Mains Road, Edinburgh, UK EH9 3JJ*
[d] *Zeneca Specialities Plc, Hexagon House, Blackley, Manchester, UK M9 3DA*

***Received 5th May 1998, Accepted 8th September 1998***

Reaction of 2,6-diformyl- and 2,6-diacetyl-4-methylphenol with a large excess of both $NH_2OH{\cdot}HCl$ and $CH_3CO_2K$ in EtOH affords high yields of 2,6-diformyl-4-methylphenol dioxime (2-hydroxy-5-methylbenzenedicarbaldehyde dioxime) ($H_3L^1$) and 2,6-diacetyl-4-methylphenol dioxime ($H_3L^2$), respectively. The crystal structure of ($H_3L^2$) shows intramolecular hydrogen bonding with long-range intermolecular π-stacking interactions and an extended intermolecular hydrogen-bonding network. The binuclear complexes of $Co^{II}$, $Ni^{II}$ and $Cu^{II}$—$[Co_2(H_2L^1)_2(MeOH)_2(H_2O)_2]Cl_2{\cdot}2MeOH$, $[Ni_2(H_2L^1)_2(H_2O)_4][ClO_4]_2{\cdot}2H_2O$ and $[Cu_2(H_2L^1)_2(ClO_4)_2]$, respectively—derived from the dioxime ligand ($H_3L^1$) have been synthesized and characterised and their single-crystal structures determined. The structure of $[Co_2(H_2L^1)_2(MeOH)_2(H_2O)_2]^{2+}$ shows each high-spin $Co^{II}$ to be six-co-ordinate and bound to an $N_2O_4$-donor array presented by two dioxime ligands and axially co-ordinated $H_2O$ and MeOH molecules, the dioxime ligands co-ordinating *via* the imino N- and phenoxy O-donors. The structure of $[Ni_2(H_2L^1)_2(H_2O)_4]^{2+}$ shows two octahedrally co-ordinated $Ni^{II}$ each with an $N_2O_4$ donor set similar to that in $[Co_2(H_2L^1)_2(MeOH)_2(H_2O)_2]^{2+}$ except that the co-ordination sphere of each $Ni^{II}$ is completed by axial ligation to two $H_2O$ molecules. The structure of $[Cu_2(H_2L^1)_2(ClO_4)_2]$ confirms $N_2O_4$ donation at $Cu^{II}$ with two bidentate $ClO_4^-$ anions, Cu ··· O 2.51(2), 2.76(2) Å, interacting with the metal centres on either side of the planar oxime–phenolate array. In all three complexes the two dioxime ligands are monodeprotonated at the phenolic oxygen, and the oximes are linked by hydrogen bonds, which results in a pseudo-macrocyclic framework. Magnetic susceptibility measurements on the complexes over the range 2.5–340 K confirm that the complexes are antiferromagnetically coupled with values for the magnetic exchange constant $J$ of $-6.9 \pm 0.1$, $-16.0 \pm 0.6$, and $-452 \pm 4$ $cm^{-1}$ for $[Co_2(H_2L^1)_2(MeOH)_2(H_2O)_2]Cl_2$, $[Ni_2(H_2L^1)_2(H_2O)_4][ClO_4]_2$ and $[Cu_2(H_2L^1)_2(ClO_4)_2]$, respectively.

## Introduction

Since the mid-1960s *ortho*-hydroxyoximes have been utilised commercially for the solvent extraction of copper from aqueous solutions of acid-soluble copper ores.[1] Such reagents bind to copper(II) ions to give a neutral 2:1 complex from which the metal is liberated by back extraction into a strongly acidic aqueous phase.[2] As part of an investigation into the solvent extractant abilities of analogous binucleating dioxime ligands we have synthesized 2,6-diformyl-4-methylphenol dioxime (2-hydroxy-5-methylbenzenedicarbaldehyde dioxime) ($H_3L^1$) and studied its reaction with various salts of $Co^{II}$, $Ni^{II}$ and $Cu^{II}$. Formation of binuclear transition complexes with oxime ligands has been observed previously, notably with $Ag^I$,[3] $Cu^{II}$ [3–5] and $Ni^{II}$.[6] There have been relatively few reports dealing with the co-ordination chemistry of 2,6-diformyl-4-methylphenol dioxime and its derivatives.[7–10] In 1973 Okawa *et al.*[7] reported the reaction of 2,6-diformyl-4-methylphenol with $NH_2OH$ in the presence of $Cu(O_2CMe)_2{\cdot}H_2O$ and $NiCl_2{\cdot}6H_2O$. In both cases insoluble complexes were obtained which, on the basis of microanalytical, magnetic susceptibility, spectroscopic and mass spectral data, were assigned the formulations $[Cu_2(HL^1)_2]$ and $[Ni_2(HL^1)_2]{\cdot}3H_2O$. Very recently, Thompson and co-workers[9] have reported magnetochemical and structural data on related nickel(II) oxime complexes, while Busch and co-workers[10] have prepared asymmetric iminooxime compartmental species. In addition, Chaudhuri and co-workers[8] have reported the reaction of $H_3L^1$ with $Ni(O_2CMe)_2{\cdot}4H_2O$ and $[FeLCl_3]$ (L = 1,4,7-trimethyl-1,4,7-triazacyclononane) in basic MeOH solution. After treatment with $Bu_4NBF_4$ a solid of formulation $[Fe_2Ni_2(\mu\text{-}O_2CMe)_2L_2(L^1)_2(MeOH)_2][BF_4]_2$ was isolated and characterised by X-ray crystallographic and magnetic susceptibility measurements. This tetranuclear complex exhibits a nearly linear $Fe^{III}Ni^{II}Ni^{II}Fe^{III}$ core in which each metal centre adopts an octahedral co-ordination geometry.

We report herein the synthesis and structures of oxime ligands derived from 2,6-diacetyl- and 2,6-diformyl-4-methylphenol, and the synthesis, structures and magnetochemistry of their complexes of $Co^{II}$, $Ni^{II}$ and $Cu^{II}$.

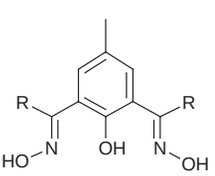


R = H: $H_3L^1$
R = Me: $H_3L^2$

## Results and discussion

Reaction of either 2,6-diformyl-4-methylphenol or 2,6-diacetyl-4-methylphenol with a large excess of both $NH_2OH·HCl$ and $CH_3CO_2K$ in EtOH affords, after aqueous work-up, high yields of 2,6-diformyl-4-methylphenol dioxime ($H_3L^1$) and 2,6-diacetyl-4-methylphenol dioxime ($H_3L^2$), respectively. The IR spectrum of $H_3L^1$ shows sharp bands at 1623 and 1604 $cm^{-1}$ assigned to the C=N stretching vibration, while $H_3L^2$ shows the corresponding absorption at 1647 $cm^{-1}$. The mass spectra of the compounds show molecular ion peaks at *m*/*z* 194 and 223, corresponding to $[H_3L^1]^+$ and $[H_3L^2 + H]^+$ respectively, while $^1H$ NMR spectroscopy of $H_3L^1$ in $(CD_3)_2CO$ shows single resonances at $\delta$ 2.27, 7.37 and 8.38 assigned to the $CH_3$, aromatic CH and imine protons respectively. Additional single resonances are observed at $\delta$ 10.48 (phenolic OH) and 10.71 (oxime OH). The $^{13}C$ DEPT NMR spectrum shows a methyl carbon resonance at $\delta$ 18.54 as well as resonances at $\delta$ 117.94 and 127.64 due to quaternary aromatic carbon centres. Resonances at $\delta$ 128.68 (aromatic CH), 146.71 (imino C) and 152.29 (COH) are also observed. These data indicate either the presence in solution of one symmetrical isomer, or a mixture of rapidly interconverting isomers. Whilst the interconversion of oxime isomers in solution has been reported,[11] steric factors would perhaps be expected to favour the formation of a *E* configuration at each C=N bond. It has not proven possible to grow crystals of $H_3L^1$ of suitable quality for crystallographic studies and so the solid-state structure of the ligand has not been established.

The $^1H$ NMR spectrum of $H_3L^2$ in $CD_3OD$ shows three single peaks. Two distinct methyl proton resonances are observed at $\delta$ 2.26 and 2.29 assigned to aliphatic and ring methyl groups respectively, while the aromatic proton resonance appears at $\delta$ 7.18. No resonances are seen for the phenolic and oxime protons because of rapid exchange with the solvent. The $^{13}C$ DEPT NMR spectrum shows methyl carbon resonances at $\delta$ 11.79 and 19.22, quaternary aromatic carbon resonances at $\delta$ 122.50 and 127.30, and an aromatic CH resonance at $\delta$ 129.32. The spectrum is completed by the COH and imino C resonances at $\delta$ 157.39 and 153.68. These spectra also indicate either the presence of one symmetrical isomer or a mixture of rapidly interconverting isomers in solution.

Pale yellow crystals of $H_3L^2$ of diffraction quality were obtained by slow evaporation from a $(CD_3)_2CO$ solution of the compound. A single-crystal structure determination was undertaken to establish which isomer of $H_3L^2$ is present in the solid state. The molecular structure confirms [Fig. 1(a), Table 1] that each C=N double bond has a *E* configuration with the oxime hydroxyl groups and the aromatic ring on opposite sides of the double bond. An intramolecular hydrogen bond is observed within each dioxime molecule between the phenolic H atom and an N-donor of the oxime group. The crystal structure reveals that the dioxime molecules associate through extensive intermolecular hydrogen bonding [Fig. 1(b)] to produce extended molecular chains. This contrasts with the structure of salicylaldoxime[12] in which only hydrogen-bonded dimers are formed. Association between adjacent chains occurs *via* long-range π-stacking interactions, the separation between adjacent ring centroids being *ca.* 3.7 Å.

### Metal complexation

**Cobalt.** Treatment of $H_3L^1$ with 1 equivalent of $CoCl_2·6H_2O$ in MeOH affords an orange solution from which an orange solid can be isolated. The FAB mass spectrum of this solid shows a peak at *m*/*z* 503, corresponding to $[^{59}Co_2(H_2L^1)_2 - H]^+$ with the correct isotopic distribution. The IR spectrum shows absorption peaks at 1636 and 1617 $cm^{-1}$ assigned to the C=N stretching vibration. In order to determine unambiguously the structure of the complex a single-crystal structure determination was undertaken. Suitable crystals were grown by slow evaporation from a MeOH solution of the complex.

**Table 1** Selected bond lengths (Å) and angles (°) with e.s.d.s for $H_3L^2$

| | | | |
|---|---|---|---|
| O(1)–C(1) | 1.368(4) | C(20)–C(21) | 1.492(5) |
| O(2)–N(2) | 1.392(4) | C(6)–C(60) | 1.495(5) |
| O(6)–N(6) | 1.407(4) | N(6)–C(60) | 1.287(5) |
| C(2)–C(20) | 1.475(5) | C(60)–C(61) | 1.480(5) |
| N(2)–C(20) | 1.288(5) | C(4)–C(40) | 1.519(5) |
| | | | |
| C(20)–N(2)–O(2) | 113.0(3) | C(2)–C(20)–C(21) | 121.3(4) |
| C(60)–N(6)–O(6) | 111.1(3) | N(6)–C(60)–C(61) | 125.3(4) |
| N(2)–C(20)–C(2) | 115.4(3) | N(6)–C(60)–C(6) | 113.5(4) |
| N(2)–C(20)–C(21) | 123.4(4) | C(61)–C(60)–C(6) | 121.1(4) |

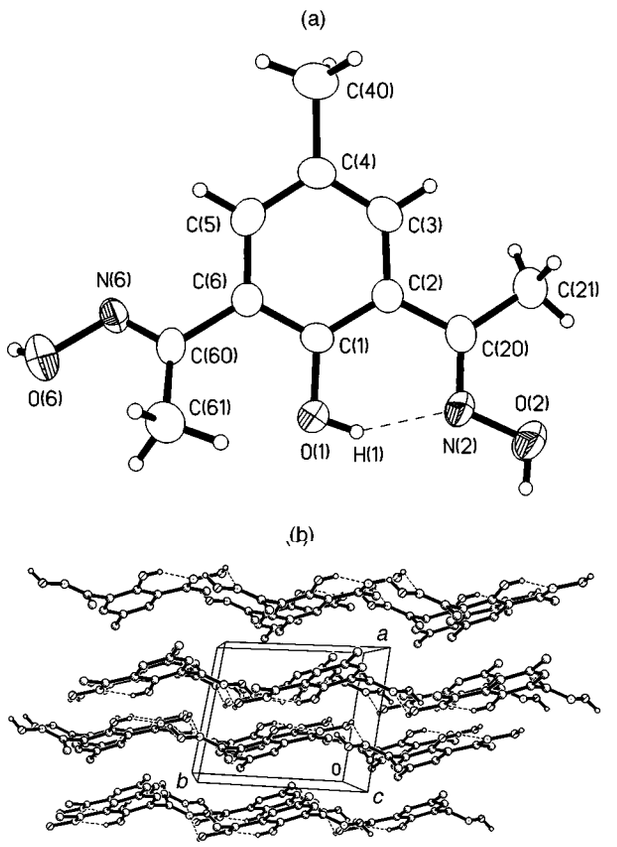


**Fig. 1** (a) View of the structure of $H_3L^2$ with numbering scheme adopted. H(1)···N(2) 1.83 Å, O(1)–H(1)–N(2) 145°, O(1)···N(2) 2.542(6) Å. (b) View of the packing diagram of $H_3L^2$.

The structure of $[Co_2(H_2L^1)_2(H_2O)_2(MeOH)_2]Cl_2·2MeOH$ shows (Fig. 2, Table 2) a centrosymmetric binuclear structure with each octahedral cobalt(II) centre bound to an $N_2O_4$-donor set from two dioxime ligands, Co–N 2.071(4), 2.073(4), Co–O 2.055(4), 2.075(4) Å, one axial $H_2O$ molecule, Co–O 2.102(4) Å, and one axial MeOH molecule, Co–O 2.133(4) Å. A crystallographic centre of inversion lies at the midpoint of the Co–Co vector, Co···Co 3.092(2) Å. The two $Co^{II}$ lie in the plane defined by the four N- and two O-donor atoms of the dioxime ligands. The complex has a pseudo-macrocyclic structure which results from hydrogen bonding between the two dioxime ligands, O(2)···O(3) 2.740(6) Å. Opposite pairs of oxime hydroxyl groups lie marginally above and below this plane as a result of accommodating this hydrogen bond.

**Nickel.** The reaction of $H_3L^1$ with a slight excess of $Ni(ClO_4)_2·6H_2O$ in thf–MeOH affords a green solution. Crystals of diffraction quality were grown directly from this solution by slow evaporation at room temperature. The FAB mass spectrum of a sample of the crystalline material shows a peak at *m*/*z* 501, corresponding to $[^{58}Ni_2(H_2L^1)_2 - H]^+$ with the correct isotopic

**Table 2** Selected bond lengths (Å) and angles (°) with e.s.d.s for $[Co_2(H_2L^1)_2(H_2O)_2(MeOH)_2]Cl_2\cdot 2MeOH$

| | | | |
|---|---|---|---|
| Co(1)–O(1) | 2.055(4) | Co(1)–O(5) | 2.102(4) |
| Co(1)–N(1) | 2.071(4) | Co(1)–O(4′) | 2.133(4) |
| Co(1)–N(2) | 2.073(4) | Co(1)···Co(1′) | 3.092(2) |
| Co(1)–O(1′) | 2.075(4) | | |
| O(1)–Co(1)–N(1) | 169.3(2) | N(2)–Co(1)–O(5) | 88.8(2) |
| O(1)–Co(1)–N(2) | 87.3(2) | O(1′)–Co(1)–O(5) | 91.6(2) |
| N(1)–Co(1)–N(2) | 103.2(2) | O(1)–Co(1)–O(4′) | 89.8(2) |
| O(1)–Co(1)–O(1′) | 83.1(2) | N(1)–Co(1)–O(4′) | 88.2(2) |
| N(1)–Co(1)–O(1′) | 86.5(2) | N(2)–Co(1)–O(4′) | 88.0(2) |
| N(2)–Co(1)–O(1′) | 170.3(2) | O(1′)–Co(1)–O(4′) | 92.7(2) |
| O(1)–Co(1)–O(5) | 96.3(2) | O(5)–Co(1)–O(4′) | 172.9(2) |
| N(1)–Co(1)–O(5) | 86.5(2) | Co(1)–O(1)–Co(1′) | 96.9(2) |

Primed atoms are related to their unprimed equivalents by the symmetry operation $(-x, -y + 1, -z)$.

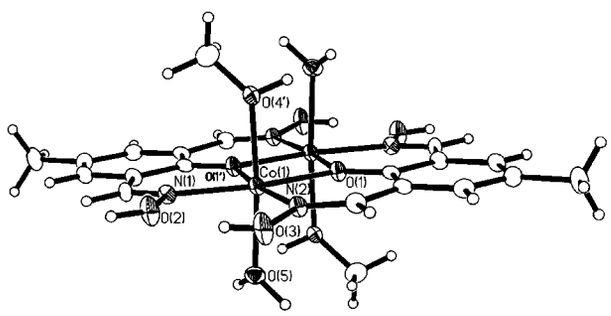


**Fig. 2** View of the structure of $[Co_2(H_2L^1)_2(H_2O)_2(MeOH)_2]^{2+}$ with numbering scheme adopted. The chloride counter anions and non-co-ordinating methanol molecules are omitted for clarity. Primed atoms are related to their unprimed equivalents by the symmetry operation $(-x, -y + 1, -z)$.

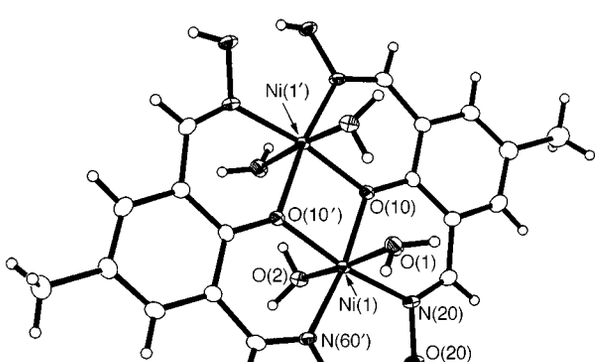


**Fig. 3** View of the structure of $[Ni_2(H_2L^1)_2(H_2O)_4]^{2+}$ with numbering scheme adopted. The perchlorate counter anions and non-co-ordinating water molecules are omitted for clarity. Primed atoms are related to their unprimed equivalents by the symmetry operation $(-x + 1, -y, -z + 1)$.

distribution. The IR spectrum of the crystalline material shows absorption bands at 1648 and 1621 $cm^{-1}$ assigned to the C=N stretching vibration. The presence of the $ClO_4^-$ counter anion was confirmed by three very intense absorptions at 1145, 1112 and 1086 $cm^{-1}$. Electronic spectroscopy suggested that the product incorporates octahedral nickel(II) centres. To establish fully the nature of the complex a single-crystal structure determination was undertaken.

The structure of $[Ni_2(H_2L^1)_2(H_2O)_4][ClO_4]_2\cdot 2H_2O$ shows (Fig. 3, Table 3) a centrosymmetric binuclear structure with both $Ni^{II}$ centres having octahedral stereochemistries. A crystallographic centre of inversion lies at the midpoint of the Ni–Ni vector. Each $Ni^{II}$ is bound to a $N_2O_4$ donor set from two dioxime ligands, Ni–N 2.012(2), 2.024(2), Ni–O 2.0167(13), 2.0206(14) Å, and to two axially co-ordinated water molecules,

**Table 3** Selected bond lengths (Å) and angles (°) with e.s.d.s for $[Ni_2(H_2L^1)_2(H_2O)_4][ClO_4]_2\cdot 2H_2O$

| | | | |
|---|---|---|---|
| Ni(1)–N(20) | 2.012(2) | Ni(1)–O(2) | 2.086(2) |
| Ni(1)–O(10) | 2.017(1) | Ni(1)–O(1) | 2.154(2) |
| Ni(1)–O(10′) | 2.021(1) | Ni(1)···Ni(1′) | 3.0495(8) |
| Ni(1)–N(60′) | 2.024(2) | | |
| N(20)–Ni(1)–O(10) | 88.70(6) | O(10′)–Ni(1)–O(2) | 90.14(6) |
| N(20)–Ni(1)–O(10′) | 170.58(6) | N(60′)–Ni(1)–O(2) | 93.51(6) |
| O(10)–Ni(1)–O(10′) | 81.88(6) | N(20)–Ni(1)–O(1) | 92.07(6) |
| N(20)–Ni(1)–N(60′) | 100.79(7) | O(10)–Ni(1)–O(1) | 88.68(6) |
| O(10)–Ni(1)–N(60′) | 170.49(6) | O(10′)–Ni(1)–O(1) | 87.85(6) |
| O(10′)–Ni(1)–N(60′) | 88.62(6) | N(60′)–Ni(1)–O(1) | 90.48(6) |
| N(20)–Ni(1)–O(2) | 89.26(6) | O(2)–Ni(1)–O(1) | 175.49(5) |
| O(10)–Ni(1)–O(2) | 87.04(6) | Ni(1)–O(10)–Ni(1′) | 98.12(6) |

Primed atoms are related to their unprimed equivalents by the symmetry operation $(-x + 1, -y, -z + 1)$.

Ni–O 2.086(2), 2.154(2) Å. These bond lengths are similar to those reported for the $Ni_2O_2N_4$ core of $[Fe_2Ni_2(\mu\text{-}O_2CMe)_2L_2\text{-}(L^1)_2(MeOH)_2][BF_4]_2$.[8] As in $[Co_2(H_2L^1)_2(H_2O)_2(MeOH)_2]Cl_2\cdot 2MeOH$, the metal ions in $[Ni_2(H_2L^1)_2(H_2O)_4]^{2+}$ lie almost in the plane defined by the four N- and two O-donor atoms of the two dioxime ligands, Ni···Ni 3.0495(8) Å. The opposing pairs of oxime hydroxyl groups lie slightly above and below this plane as a result of accommodating a hydrogen bond, $O(20)\cdots O(60^i)$ 2.634(3) Å, i $1 - x, -y, 1 - z$, between them. Again, this association results in the complex having a pseudo-macrocyclic structure. Such linkages between oxime hydroxyl groups have been reported previously.[5,13] In addition, there is a hydrogen bond between the two water molecules above each face of the complex.

Reaction between $H_3L^1$ and other nickel(II) salts such as $NiCl_2\cdot 2H_2O$ and $Ni(O_2CMe)_2\cdot 4H_2O$ affords extremely insoluble pale green solids in all cases. The FAB mass spectral data indicate the presence of $[Ni_2(H_2L^1)_2]^{2+}$ units within these products. We speculate that the marked insolubility of these solids arises either from the presence of a very extensive hydrogen-bonding network within the structure, or from stacking of the binuclear $Ni^{II}_2$ complexes such that each $Ni^{II}$ achieves an octahedral co-ordination by axial ligation of hydroxyl oxygen atoms from adjacent oxime groups. These observations concerning the relative insolubility of these compounds are in accord with those reported by Okawa *et al.*[7]

**Copper.** We have found that reaction between $H_3L^1$ and a range of copper(II) salts affords similarly insoluble solids. The FAB mass spectral data indicate the presence of binuclear $[Cu_2(H_2L^1)_2]^{2+}$ units within these materials although the precise nature of these products is unknown.

One equivalent of $H_3L^1$ was dissolved in thf. The solution was frozen and then allowed to thaw by gradual warming to room temperature. A solution of 2 equivalents of $Cu(ClO_4)_2\cdot 6H_2O$ in MeOH was added to the freshly thawed thf solution of $H_3L^1$. Stirring of the pale green solution overnight at room temperature led to the precipitation of a khaki-green solid which was collected, washed with diethyl ether and dried under suction. The IR spectrum of the product shows absorptions at 1612 and 1592 $cm^{-1}$ which are assigned to C=N bond stretching vibrations, and also reveals the presence of $ClO_4^-$ counter ions. However, the FAB mass spectrum of the material did not show any peaks which could be assigned conclusively.

Crystals of this product were grown from thf–MeOH solution. A single crystal structure determination confirms (Fig. 4, Table 4) a binuclear species $[Cu_2(H_2L^1)_2(ClO_4)_2]$ with both $Cu^{II}$ centres displaying octahedral co-ordination geometries. The two dioxime ligands and the two $Cu^{II}$ form an approximately planar array. A crystallographic two-fold axis passes through the methyl carbons and phenolate oxygens which results in there being only two independent Cu–N and two independent

**Table 4** Selected bond lengths (Å) and angles (°) with e.s.d.s for $[Cu_2(H_2L^1)_2(ClO_4)_2]\cdot 2thf$

| | | | |
|---|---|---|---|
| Cu–O(1A) | 1.941(10) | Cu–N(1B) | 1.99(2) |
| Cu–N(1A) | 1.95(2) | Cu···Cu′ | 2.994(4) |
| Cu–O(1B) | 1.965(12) | | |
| N(1A)–Cu–N(1B) | 100.2(7) | N(1A)–Cu–O(1A) | 90.5(6) |
| O(1A)–Cu–O(1B) | 79.9(5) | O(1A)–Cu–N(1B) | 166.1(6) |
| N(1A)–Cu–O(1B) | 167.9(6) | Cu–O(1A)–Cu′ | 100.9(7) |
| N(1B)–Cu–O(1B) | 90.5(7) | Cu–O(1B)–Cu′ | 99.2(8) |

Primed atoms are related to their unprimed equivalents by the symmetry operation $(x, \frac{1}{2} - y, \frac{1}{4} - z)$.

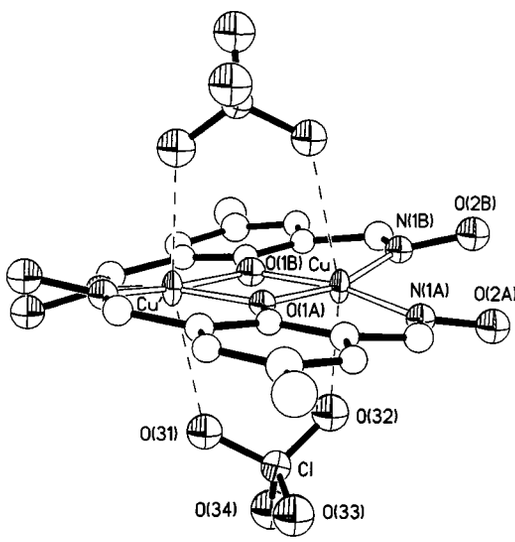


**Fig. 4** View of the structure of $[Cu_2(H_2L^1)_2(ClO_4)_2]$ with numbering scheme adopted. Non-co-ordinating thf molecules are omitted for clarity. Primed atoms are related to their unprimed equivalents by the symmetry operation $(x, \frac{1}{2} - y, \frac{1}{4} - z)$.

Cu–O distances (Table 4), Cu–N 1.95(2), 1.99(2) Å; Cu–O (phenoxy) 1.941(10), 1.965(12) Å, and which dictates that the $Cu_2O_2$ core is planar. The estimated standard deviations (e.s.d.s) are relatively high due to crystal decomposition during data collection and solvent disorder, but it is clear that these bond lengths are slightly shorter than those observed in the structures of $[Ni_2(H_2L^1)_2(H_2O)_4][ClO_4]_2\cdot 2H_2O$ and $[Co_2(H_2L^1)_2(MeOH)_2(H_2O)_2]Cl_2\cdot 2MeOH$. The Cu···Cu separation is 2.994(4) Å and the two Cu–O–Cu angles are 99.2(8) and 100.9(7)°. Two symmetry-related bidentate $ClO_4^-$ anions bridge in an asymmetric manner between the two $Cu^{II}$, one above and one below the plane of the hydroxydioxime ligands, Cu–O ($ClO_4^-$) 2.51(2), 2.76(2) Å. This co-ordination mode has been found for many related perchlorate complexes.[14] The elongated axial interactions demonstrate the Jahn–Teller distortion expected for octahedrally co-ordinated $Cu^{II}$. Opposing pairs of hydroxyl groups lie fractionally above and below the plane of the two hydroxydioxime ligands and are linked *via* an intramolecular hydrogen bond, O(2A)···O(2B) 2.59(3) Å. Two severely disordered thf solvent molecules accompany each complex.

## Magnetic measurements

**Nickel.** The molar magnetic susceptibility of $[Ni_2(H_2L^1)_2(H_2O)_4][ClO_4]_2\cdot 2H_2O$ was measured over the temperature range 2.5–340 K. The data are displayed in Fig. 5. The distinct cusp at about 40 K indicates significant antiferromagnetic exchange and the secondary rise in susceptibility at lower temperatures implies that there is a small amount of a paramagnetic impurity.

One expects that the electronic ground state of $Ni^{II}$ in an octahedral, or slightly distorted octahedral, ligand field has

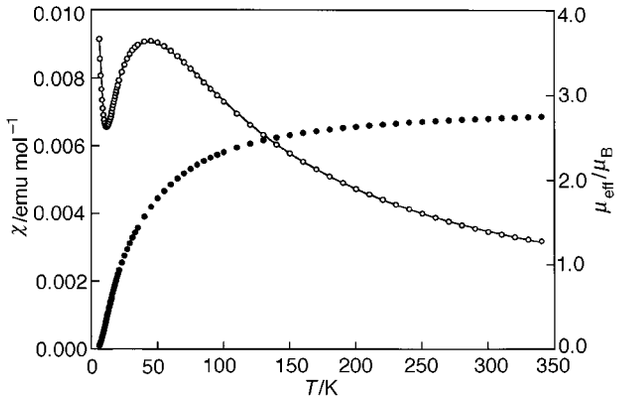


**Fig. 5** Molar magnetic susceptibility per $Ni^{II}$ for $[Ni_2(H_2L^1)_2(H_2O)_4][ClO_4]_2\cdot 2H_2O$ (open circles) with a fit by the expression for a dimer of exchange-coupled spins $S = 1$ with a zero-field splitting $D$ as described in the text. Closed circles denote the effective moment per $Ni^{II}$ ion.

electronic spin $S = 1$, and that the susceptibility $\chi$ will be described well by the appropriate expression for an exchange coupled dimer with isotropic exchange. The data for $[Ni_2(H_2L^1)_2(H_2O)_4][ClO_4]_2\cdot 2H_2O$ were fitted by least squares using eqn. (1) where $\chi$ is defined per mol of $Ni^{II}$ in the sample, $\rho$ is the

$$\chi = (1 - \rho)\frac{C}{T}F(J,T) + \rho\frac{C'}{T} + \chi_{TIP} \qquad (1)$$

fraction of a paramagnetic nickel(II) impurity with Curie constant $C'$, and $J$ is the intramolecular exchange constant for the binuclear complex, defined for the isotropic exchange Hamiltonian (2). For $S = 1$, $C = Ng^2\beta^2/k$, and $F(J,T) = (2e^{2x} + 10e^{6x})/(1 + 3e^{2x} + 5e^{2x})$, where $x = J/kT$; $\chi_{TIP}$ represents any temperature independent paramagnetism, arising from the second-order Zeeman effect, and is of the order of $240 \times 10^{-6}$ emu mol$^{-1}$. A least-squares fit of expression (1) to the data over the full temperature range yielded $J = -17.3 \pm 0.6$ cm$^{-1}$, $g = 2.06 \pm 0.01$ and $\rho = 0.03 \pm 0.003$, while the TIP contribution was found to be $(2.9 \pm 0.1) \times 10^{-5}$ emu mol$^{-1}$.

$$H = -2J\, S_1\cdot S_2 \qquad (2)$$

The susceptibility of a series of binuclear nickel(II) complexes with similar co-ordination and geometry has been treated recently in some detail,[9] and it has been shown that further influences on the form of the susceptibility may also need to be taken into account. In particular, the non-cubic components of the ligand field may act on the $S = 1$ ground state to produce a zero-field splitting which may be of the same order of magnitude as $J$.[15,16] We fitted our data using the explicit expression[9] for a dimer of $S = 1$ ions with a zero-field splitting $D$ and intramolecular dimer exchange $J$. The optimised values of $D$ and $J$ were $17.9 \pm 0.9$ cm$^{-1}$ and $-16.0 \pm 0.6$ cm$^{-1}$ respectively. It is conceivable that there is also an intermolecular exchange interaction $J'$ which will perturb the optimised values of $D$ and $J$. However, there was little improvement in fit when $J'$ was introduced. In the absence of evidence for such an effect, or any obvious structural feature suggesting that interdimer exchange should be significant, we chose not to explore this possibility further with more sophisticated fitting procedures. The results when $J'$ is set to zero are reproduced in Fig. 5.

**Cobalt.** Samples of $[Co_2(H_2L^1)_2(MeOH)_2(H_2O)_2]Cl_2\cdot 2MeOH$ could be prepared as crystals sufficiently large for single crystal magnetic susceptibility measurements. Measurements were made on a flat piece of this material mounted on a silica strand with nail varnish over the temperature range 2.5–290 K. The susceptibility of the sample was found not to change signifi-

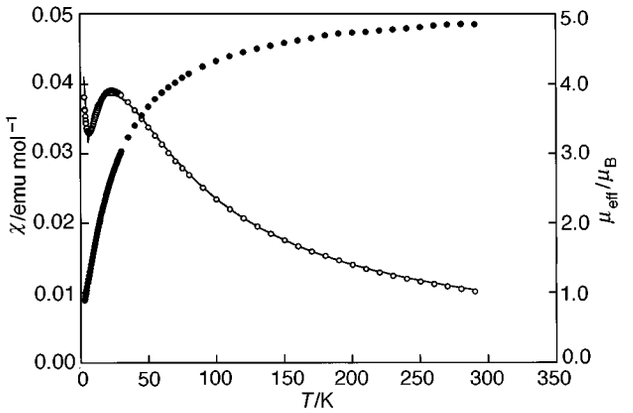


**Fig. 6** Molar magnetic susceptibility per $Co^{II}$ for $[Co_2(H_2L^1)_2(MeOH)_2(H_2O)_2]Cl_2\cdot 2MeOH$ (open circles) with a fit by the expression [eqns. (1) and (3)] for a dimer of exchange-coupled spins $S = \frac{3}{2}$ as described in the text. Closed circles denote the effective moment per $Co^{II}$.

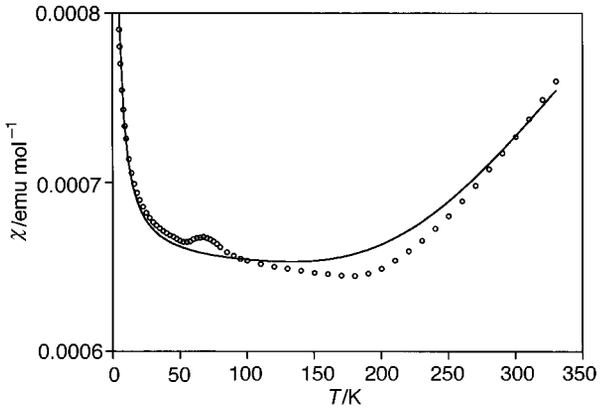


**Fig. 7** Molar magnetic susceptibility per $Cu^{II}$ for $[Cu_2(H_2L^1)_2(ClO_4)_2]\cdot 2thf$ (open circles) with a fit by a modified Bleaney–Bowers expression [eqns. (1) and (4)] for a dimer of spins $S = \frac{1}{2}$ with $g$ fixed at 2.40. The feature centred at approximately 70 K is assumed to be an impurity and so data over the temperature range 40–100 K were not included in the fitting procedure.

cantly with its orientation for three different settings relative to the flat plane of the flake, and a separate measurement on a powder sample held in a gelatine capsule yielded very similar data. The data are displayed in Fig. 6. The cusp centred at approximately 20 K indicates significant antiferromagnetic exchange, and the secondary rise in the susceptibility at lower temperatures implies that a paramagnetic impurity is present.

The $3d^7$ configuration of $Co^{II}$ in a octahedral ligand field and in a high-spin state has a $^4T_1$ ground term which bestows an orbital contribution on the moment, raising it from the spin-only value of $\sqrt{15}\mu_B$ to a value that lies typically in the range 4.5–5.1$\mu_B$.[15] The precise calculation of the moment not only requires reliable values of ligand-field and spin–orbit coupling parameters, but also of the degree of electron delocalisation, and we treat it here merely as an empirical term to be estimated from our data. The molar susceptibility data were fitted by the expression (3) used for the binuclear nickel(II) complex with

$$F(J,T) = \frac{(2e^{2x} + 10e^{6x} + 28e^{12x})}{(1 + 3e^{2x} + 5e^{6x} + 7e^{12x})} \quad (3)$$

$F(J,T)$ modified for two centres each of spin $S = \frac{3}{2}$. The least-squares fit yielded the values $J = -6.9 \pm 0.1$ cm$^{-1}$, $g = 2.49 \pm 0.05$ and $\rho = 0.03 \pm 0.0006$, assuming the paramagnetic impurity to have a similar effective moment as the cobalt(II) ions in the binuclear complex. This value of $g$ yields a moment of 4.82$\mu_B$, which is in the range of typical values given above for high-spin $Co^{II}$ in an octahedral field. The fit and the dependence of the effective moment on temperature are displayed in Fig. 6. Deviations of the susceptibility from the theoretical expression probably reflect the effect of single-ion anisotropy[15,17] or anisotropic exchange,[18] both of which are likely to be significant for a $^4T_1$ term subjected to non-cubic structural distortions.

**Copper.** The molar magnetic susceptibility of a powder sample of $[Cu_2(H_2L^1)_2][ClO_4]_2\cdot 2thf$ was measured over the temperature range 2.5–330 K. The data are displayed in Fig. 7. The magnitude of the effective moment is very small[7] except at the highest temperatures where the susceptibility rises on warming. This implies that the exchange coupling in the binuclear complex is strong and that the cusp in susceptibility lies well above the maximum experimental temperature. There was also a very small contribution to the susceptibility at lower temperatures, reflecting the presence of a small amount of paramagnetic impurity. Finally, a weak cusp centred at about 70 K reflects a small concentration of an unidentified impurity. We regard contamination with $O_2$ as unlikely since this feature is not observed in the absence of the sample, it is not observed for other complexes investigated in the present study, and it appears to be a consistent feature for this particular complex.

The $3d^9$ configuration of $Cu^{II}$ in an octahedral ligand has a $^2E_1$ ground term with a magnetic moment given approximately by the spin-only value of $\sqrt{3}\mu_B$; perturbation by spin–orbit coupling with excited ligand-field states and a second-order Zeeman contribution modify this value to lie typically in the range 1.9–2.0$\mu_B$.[15] The molar susceptibility data were fitted by expression (1) used for the $Ni^{II}_2$ complex with $F(J,T)$ modified for a dimer of spins $S = \frac{1}{2}$, *i.e.* as in eqn. (4).

$$F(J,T) = \frac{2e^{2x}}{(1 + 3e^{2x})} \quad (4)$$

Data in the region 40–100 K were not included in the fitting procedure because we did not know what to use to model the feature at 70 K. It should be noted, however, that the removal of this portion of the data did not have a significant influence on the fit at higher temperatures. It was not possible to produce a stable fit to the data if both $J$ and the effective moment were unconstrained, so we fixed the $g$ value for the moments in the dimer to be 2.00, 2.20 and 2.40, spanning a range of values observed for binuclear copper(II) species.[17] In all cases the TIP contribution was found to be $0.00064 \pm 0.00002$ emu mol$^{-1}$, and the fraction of paramagnetic impurity (assumed to be monomeric $Cu^{II}$ with $g = 2.00$) to be 0.20(1)%. Values of $J$ of $-415 \pm 5$, $-435 \pm 5$ and $-452 \pm 4$ cm$^{-1}$ were found for $g = 2.00$, 2.20 and 2.40 respectively. The X-band EPR spectrum of this complex is consistent with relatively strong antiferromagnetic coupling with a very broad signal being observed. The value for TIP is anomalously high, values of approximately 0.00006 emu mol$^{-1}$ being more typical. The feature at 70 K will have some contribution to this term in the fit, but is unlikely to account in full for this discrepancy.

### Magnetostructural trends in metal(II) dioxime complexes

Magnetostructural correlations in dimeric transition metal compounds have been extensively studied and rationalised,[19] particularly in the case of copper(II) ions linked through hydroxide ions.[20] Detailed analysis of the relation between $J$ and the structure and bonding in the compound requires a thorough consideration of the MOs constructed from valence orbitals on the metal ions and mediating ligands and is beyond the scope of this paper, so we will confine our discussion to a comparison with related compounds and general features of the magnetochemistry. The net exchange in all these materials is composed of competing ferro- and antiferro-magnetic

**Table 5** Magnetic and structural parameters

| Complex | $J$/cm$^{-1}$ | $S$ | $4JS^2$/cm$^{-1}$ | M–O/Å | M···M/Å | M–O–M/° |
|---|---|---|---|---|---|---|
| $[Co_2(H_2L^1)_2(H_2O)_2(MeOH)_2]Cl_2\cdot 2MeOH$ | −6.9 | $\frac{3}{2}$ | −62.1 | 2.055(4), 2.075(4) | 3.092(2) | 96.9(2) |
| $[Ni_2(H_2L^1)_2(H_2O)_4][ClO_4]_2\cdot 2H_2O$ | −16.0 | 1 | −72 | 2.017(1), 2.021(1) | 3.0495(8) | 98.12(6) |
| $[Cu_2(H_2L^1)_2(ClO_4)_2]\cdot 2thf$ | −452 | $\frac{1}{2}$ | −452 | 1.941(10), 1.965(12) | 2.994(4) | 99.2(8), 100.9(7) |

components. The antiferromagnetic component arises from the formation of MOs primarily involving σ bonding between valence orbitals on M and O, and differences in the energy of these orbitals favours pairing of electrons to form a spin singlet. In this series of binuclear complexes the principal interaction will involve p orbitals on O and $d_{x^2-y^2}$ on M, for which, in the first approximation, the MOs will be degenerate when the bridging angle $\theta$ is 90° and hence there will be no antiferromagnetic term. In principle, however, accidental orthogonality should occur at higher angles due to s–p orbital mixing. This is compounded by a ferromagnetic term arising from quantum mechanical exchange of electrons which is independent of $\theta$ to a first approximation. Thus, as $\theta$ is either raised or lowered from 90° a crossover from ferro- to antiferro-magnetic $J$ is expected at an angle that will depend, among other factors, on the strength of the M–O covalent bond and on the particular orbitals that contribute to the MOs.

In the case of binuclear copper(II) complexes linked through two phenoxide bridges, $J$ is found empirically to depend on $\theta$ above 90° as $J$ (cm$^{-1}$)= $-15.98\theta$ (degrees) + 1231[21] while the expression for a series of phenoxide-coupled nickel(II) dimers approximates to $J$ (cm$^{-1}$) = $-7.4\theta$ (degrees) + 720.[22] These expressions predict $J = -6$ and $-360$ cm$^{-1}$ respectively for the binuclear complexes of $Ni^{II}$ and $Cu^{II}$ described herein, with deviations from these predicted values anticipated on the grounds that $J$ will also depend on other ligands present and on the precise co-ordination geometry of the metal ion. In the case of the copper(II) complex this interpretation should be treated with caution. It has been pointed out[21] that the empirical relation between $\theta$ and $J$ predicts that the ferro- to antiferro-magnetic crossover will occur at $\theta = 79°$ for diphenoxy-bridged species, quite different from the universal value of 97–97.5° observed in other O-bridged $Cu^{II}$ dimers.[9,10,21,23] The complexes in the present study involve diphenoxide bridges as part of a larger tetraimino pseudo-macrocycle. This may provide an alternative exchange pathway through the conjugated π framework of the azomethine nitrogen and the benzene ring.[10] Such a term should also be antiferro-magnetic. Thus, it is possible that the phenoxide linkage in isolation would cross from ferro- to antiferro-magnetic exchange at an angle similar to that for other Cu–O–Cu dimers.

There is far less work published on binuclear cobalt(II) complexes of this or indeed any sort, and no such empirical relations between $J$ and $\theta$ have been drawn up; small values of $J$ have been observed in related exchange-coupled dimers.[24] It should be noted that a true comparison for ions with different numbers of unpaired electrons requires us to consider the quantity $4JS^2$,[25] and this term is given in Table 5 together with appropriate bond lengths and bridging angles. The increase in $4JS^2$ with atomic number reflects the increase in M–O bond strength, supplemented by the increase in M–O–M angle. Further, as the number of singly occupied d orbitals increases from $Cu^{II}$ to $Ni^{II}$ to $Co^{II}$, so too does the ferromagnetic contribution to the exchange, consistent with the observed value of $J$ in the current study.

Current work is aimed at the study of these and related systems in order to probe magnetochemical–structural correlations in polynuclear macrocyclic complexes.

## Experimental

Infrared spectra were recorded as KBr discs using a Perkin-Elmer 1600 Series FTIR spectrometer over the range 400–4000 cm$^{-1}$. Microanalyses were performed by the Edinburgh University and Nottingham University Chemistry Department Microanalytical Services. Proton and $^{13}$C NMR spectra were recorded on Bruker WP250, WP300 and WH300 instruments, fast atom bombardment (FAB) and electron impact (EI) mass spectra on a Kratos 50TC spectrometer with FAB spectra run using a 3-nitrobenzyl alcohol matrix. The molar magnetic susceptibilities of the complexes were measured using a Quantum Design $MPMS_2$ SQUID magnetometer with an applied magnetic field of 0.1 T. The data were corrected for the diamagnetic contributions of the gelatine sample holder and of the constituent atoms.[26]

2,6-diformyl-4-methylphenol[27] and 2,6-diacetyl-4-methylphenol[28] were prepared by the literature methods. All solvents were of reagent grade and were used as received.

### Synthesis of 2,6-diformyl-4-methylphenol dioxime ($H_3L^1$)

To a solution of 2,6-diformyl-4-methylphenol (0.255 g, 1.55 mmol) in EtOH (100 cm$^3$) were added $NH_2OH\cdot HCl$ (1.084 g, 15.60 mmol) and $CH_3CO_2K$ (1.529 g, 15.58 mmol). The system was refluxed for 3 h during which time the inorganic solids remained in suspension. The mixture was allowed to cool to room temperature prior to removal of the inorganic solids by filtration. Concentration of the filtrate by rotary evaporation followed by addition of deionised water resulted in the precipitation of a white solid which was collected by filtration and dried under suction. Yield = 70%. The product was purified by chromatography on silica (Merck, Kieselgel 60) using $CH_2Cl_2$–$(CH_3)_2CO$ (2:1 v/v) as eluent (Found: C, 55.67; H, 5.00; N, 14.20. Calc. for $C_9H_{10}N_2O_3$: C, 55.67; H, 5.15; N, 14.43%). EI mass spectrum: *m*/*z* 194 (100%); Calc. for $[C_9H_{10}N_2O_3]^+$ 194. $^1$H NMR [250.13 MHz, $(CD_3)_2CO$, 298 K]: $\delta$ 2.27 (s, $CH_3$, 3 H), 7.37 (s, aromatic CH, 2 H), 8.38 [s, C(NOH)*H*, 2 H], 10.48 (s, phenolic OH, 1 H) and 10.71 (s, oxime OH, 2 H). $^{13}$C DEPT NMR [62.90 MHz, $(CD_3)_2CO$, 298 K]: $\delta$ 18.54 ($CH_3$), 117.94, 127.63 (quaternary aromatic), 128.68 (aromatic CH), 146.71 [C(NOH)H] and 152.29 (COH). IR (KBr disc): 3293 (br) vs, 2919w, 1623m, 1604m, 1464s, 1377m, 1307s, 1265s, 1222w, 1176w, 1061s, 1027s, 974m, 934s, 863m, 793s, 745s, 697s and 569w cm$^{-1}$.

### Synthesis of 2,6-diacetyl-4-methylphenol dioxime ($H_3L^2$)

The method used was as above except that it was not necessary to purify the final product by chromatography. Yield = 62% (Found: C, 59.61; H, 6.39; N, 12.60. Calc. for $C_{11}H_{14}N_2O_3$: C, 59.46; H, 6.31; N, 12.61%). FAB mass spectrum: *m*/*z* 223 (100%); Calc. for $[C_{11}H_{14}N_2O_3 + H]^+$ 223. $^1$H NMR (300.13 MHz, $CD_3OD$, 298 K): $\delta$ 2.26 [s, C(NOH)C$H_3$, 6 H], 2.29 (s, $CH_3$, 3 H) and 7.18 (s, aromatic CH, 2 H). $^{13}$C DEPT NMR (75.48 MHz, $CD_3OD$, 298 K): $\delta$ 11.79, 19.22 ($CH_3$), 122.50, 127.32 (quaternary aromatic), 129.32 (aromatic CH), 153.68, 157.39 [COH and *C*(NOH)$CH_3$]. IR spectrum (KBr disc): 3376 (br) s, 2922w, 1773w, 1647s, 1612w, 1452vs, 1368s, 1342m, 1300w, 1265vs, 1249vs, 1204w, 1190s, 1103w, 1035s, 957vs, 912m, 899m, 867m, 831m, 790vs, 724m, 684s, 600m, 576m and 518w cm$^{-1}$.

### Single-crystal structure determination of 2,6-diacetyl-4-methylphenol dioxime ($H_3L^2$)

Slow evaporation of a $(CD_3)_2CO$ solution of the compound

**Table 6** Summary of crystal data

| | | | | |
|---|---|---|---|---|
| Formula | $C_{11}H_{14}N_2O_3$ | $C_{18}H_{26}Cl_2N_4Ni_2O_{18}\cdot 2H_2O$ | $C_{20}H_{30}Co_2N_4O_{10}\cdot 2CH_3OH$ | $C_{18}H_{18}Cl_2Cu_2N_4O_{14}\cdot 2C_4H_8O$ |
| $M$ | 222.24 | 810.78 | 739.32 | 818.45 |
| Crystal system | Triclinic | Monoclinic | Triclinic | Tetragonal |
| Space group | $P\bar{1}$ | $P2_1/c$ | $P\bar{1}$ | $I\bar{4}2d$ |
| $a$/Å | 7.707(2) | 8.672(2) | 9.033(6) | 21.527(3) |
| $b$/Å | 8.574(3) | 10.565(2) | 9.224(5) | 21.527(3) |
| $c$/Å | 9.597(2) | 16.568(2) | 10.085(6) | 14.759(8) |
| $\alpha$/° | 108.56(2) | | 71.26(2) | |
| $\beta$/° | 110.70(2) | 89.91(2) | 82.69(3) | |
| $\gamma$/° | 92.07(2) | | 71.90(4) | |
| $U$/Å$^3$ | 554.4 | 1518 | 756 | 6839 |
| $Z$ | 2 | 2 | 1 | 8 |
| $\mu$(Mo-K$\alpha$)/mm$^{-1}$ | 0.098 | 1.51 | 1.34 | 1.471 |
| $T$/K | 298 | 150 | 150 | 295 |
| Reflections used | 1463 | 3468 | 1934 | 1031 |
| Parameters refined | 149 | 229 | 204 | 135 |
| $R1$, $wR2$ (SHELXL 93)[a] | 0.0545, 0.162 | 0.0284, 0.0726 | 0.0407, 0.104 | |
| $R$, $R'$ (SHELX 76)[b] | | | | 0.0753, 0.0727 |

[a] $R1$ is based on $F \geqslant 4\sigma(F)$, $wR2$ on all $F^2$ data. [b] $R$ and $R'$ are based on data with $F \geqslant 5\sigma(F)$.

afforded yellow crystals of diffraction quality. The selected crystal was mounted on a Stoe Stadi-4 four-circle diffractometer (Table 6). The structure was solved by direct methods using SHELXS 86[29] and refined on $F^2$ using SHELXL 93.[30] All non-H atoms were refined with anisotropic thermal parameters and all H atoms were located from $\Delta F$ synthesis introduced at calculated positions and refined as part of a rigid group or using a riding model.

### Synthesis of $[Ni_2(H_2L^1)_2(H_2O)_4][ClO_4]_2\cdot 2H_2O$

A solution of $Ni(ClO_4)_2\cdot 6H_2O$ (0.119 g, 0.35 mmol) dissolved in MeOH (8 cm$^3$) was layered on top of a frozen solution of 2,6-diformyl-4-methylphenol dioxime (0.063 g, 0.32 mmol) in thf (8 cm$^3$), contained in a Schlenk tube. The whole system was frozen by immersion in liquid nitrogen, placed in an empty narrow-necked dewar and allowed slowly to warm to room temperature. Thawing and mixing of the two solutions resulted in the formation of a green solution. Crystalline $[Ni_2(H_2L^1)_2(H_2O)_4][ClO_4]_2\cdot 2H_2O$ was obtained by slow evaporation of the MeOH–thf. Yield = 65%. FAB mass spectrum: $m/z$ 501 (100%); Calc. for $[^{58}Ni_2(H_2L^1)_2 - H]^+$ 501 with correct isotopic distribution. IR (KBr disc): 3322 (br) s, 3114 (br) w, 1648m, 1621s, 1560s, 1508m, 1440vs, 1353m, 1316vs, 1270w, 1234s, 1145vs, 1112vs, 1086vs, 984s, 869w, 814s, 772m, 700s, 637s, 529m and 502m cm$^{-1}$. Electronic spectrum (in $CH_3CN$): $\lambda_{max}$ 560 ($\varepsilon_{max}$ = 15), 365 (9210), 254 (49630) and 209 nm (38340 dm$^3$ mol$^{-1}$ cm$^{-1}$).

### Single-crystal structure determination of $[Ni_2(H_2L^1)_2(H_2O)_4][ClO_4]_2\cdot 2H_2O$

Slow evaporation of the thf–MeOH solution of the complex afforded large, rust-brown block-like crystals. A lath was cut from one of these large crystals and sealed in a Lindemann glass capillary tube to prevent decomposition. The crystal was cooled to 150 K using an Oxford Cryosystems open-flow cryostat[31] mounted on a Stoe Stadi-4 four-circle diffractometer (Table 6). The structure was solved by direct methods using SHELXS 86[29] and refined on $F^2$ using SHELXL 93.[30] All non-H atoms were refined with anisotropic thermal parameters. The H atoms on the $H_2O$ of crystallisation and the co-ordinated $H_2O$ were located in a difference map following several cycles of least squares weighted towards high-angle data and then refined with restraints on O–H distances and H–O–H angles and with $U_{iso}(H) = 1.2U_{eq}(O)$. All other H atoms were placed geometrically or located from difference maps and refined as rigid groups or using a riding model.

### Synthesis of $[Co_2(H_2L^1)_2(MeOH)_2(H_2O)_2]Cl_2\cdot 2MeOH$

To a solution of 2,6-diformyl-4-methylphenol dioxime (0.147 g, 0.76 mmol) dissolved in MeOH (30 cm$^3$) was added $CoCl_2\cdot 6H_2O$ (0.180 g, 0.76 mmol). On dissolution of the $CoCl_2\cdot 6H_2O$ an orange solution was produced which was stirred overnight. Removal of the MeOH by rotary evaporation afforded an emerald green solid. This partially redissolved on the addition of more MeOH to afford an orange solid suspended in an orange solution. The addition of deionised water caused the orange solid to flocculate. The solid was collected by filtration, washed with the mother-liquor and dried *in vacuo*. Yield = 60% {Found: C, 40.23; H, 3.73; N, 10.24. Calc. for $[Co_2(H_2L^1)_2(MeOH)_2(H_2O)_2]Cl_2\cdot H_2O$: C, 40.47; H, 3.77; N, 10.49%}. FAB mass spectrum: $m/z$ 503 (45%); Calc. for $[^{59}Co_2(H_2L^1)_2 - H]^+$ 503 with correct isotopic distribution. IR (KBr disc): 3342vs, 3119s, 3002s, 2931s, 2778m, 1636m, 1617s, 1554vs, 1499m, 1443vs, 1350m, 1319vs, 1272w, 1234vs, 1193w, 1073m, 980vs, 872w, 812m, 767m, 697m, 637w, 518m and 501m cm$^{-1}$.

### Single-crystal structure determination of $[Co_2(H_2L^1)_2(MeOH)_2(H_2O)_2]Cl_2\cdot 2MeOH$

Slow evaporation of a MeOH solution of the complex afforded small orange block-like crystals of diffraction quality. The determination was carried out as for the previous compound.

### Synthesis of $[Cu_2(H_2L^1)_2(ClO_4)_2]\cdot 2thf$

A solution of 2,6-diformyl-4-methylphenol dioxime (0.1164 g, 0.60 mmol) in thf (20 cm$^3$) was added to a 100 cm$^3$ beaker and frozen by careful immersion of the beaker in liquid $N_2$. The frozen solution was allowed to thaw by warming to room temperature. To the freshly thawed solution of 2,6-diformyl-4-methylphenol dioxime was added a solution of $Cu(ClO_4)_2\cdot 6H_2O$ (0.2488 g, 0.67 mmol) in MeOH (20 cm$^3$). The solution was stirred overnight at room temperature during which time a khaki-green solid precipitated. This was collected, washed with diethyl ether and dried under suction. Yield = 40% {Found: C, 34.3; H, 3.6; N, 6.6. Calc. for $[Cu_2(H_2L^1)_2(ClO_4)_2]\cdot 2thf$: C, 34.5; H, 4.0; N, 6.5%}. IR (KBr disc): 3260, 1642, 1628, 1612, 1592, 1370, 1350, 1313, 1268, 1243, 1200, 1100, 1003, 972, 956, 922, 882, 820, 762, 708, 682, 564 and 514 cm$^{-1}$.

### Single-crystal structure determination of $[Cu_2(H_2L^1)_2(ClO_4)_2]\cdot 2thf$

Crystals of diffraction quality were obtained from thf–methanol solution. The selected crystals were coated in araldite resin and mounted on a Phillips PW1100 four-circle diffractometer. Owing to crystal decay, data from two crystals were collected and merged (Table 6). The structure was solved for the copper atoms by heavy-atom methods using SHELX 76:[32] the

remaining atoms were located in successive Fourier-difference syntheses and the structure was refined on *F* using SHELX 76.[32] The Cu and Cl atoms were refined with anisotropic thermal parameters. The H atoms on carbons were introduced at calculated positions and allowed to ride at a fixed distance of 1.08 Å, while two alternative sites for each of the hydroxyl H atoms were located in a Fourier-difference map. These were positionally refined with site occupation factors of 0.5.

CCDC reference number 186/1155.

### Synthesis of $[Cu_2(HL^1)_2]$

A solution of 2,6-diformyl-4-methylphenol dioxime (0.1 g, 0.52 mmol) in dmf (50 $cm^3$) was added to a solution of $[Cu(O_2CMe)_2]$ (0.24 g, 1.2 mmol) in dmf to produce a light coloured precipitate. The reaction solution was filtered and dried to give green microcystals of the product. The solution was stirred overnight at room temperature during which time a khaki-green solid precipitated. Yield = 90% {Found: C, 41.8; H, 3.4; N, 10.9. Calc. for $[Cu_2(HL^1)_2]$: C, 42.1; H, 3.4; N, 10.9%}. IR (KBr disc): 3450, 3025, 3005, 2930, 1620, 1600, 1588, 1402, 1350, 1302, 1237, 1190, 1098, 1070, 1010, 960, 930, 906, 865, 822, 762, 707, 686, 582, 568, 519, 504, 477 and 430 $cm^{-1}$.

## Acknowledgements

We thank Zeneca Specialties plc for a CASE Award (to D. B.), the EPSRC for support and the EPSRC National Mass Spectometry Service, University of Swansea. We thank the referees for helpful comments and suggestions.

## References

1 *Comprehensive Co-ordination Chemistry*, eds. G. Wilkinson, R. D. Gillard and J. A. McCleverty, Pergamon, Oxford, 1987, vol. 6.
2 B. McCudden, P. O'Brien and J. R. Thornback, *J. Chem. Soc., Dalton Trans.*, 1983, 2043; *Hydroxyoximes and Copper Hydrometallurgy*, CRC Press, Boca Raton, FL, 1993.
3 S. O. Sommerer, B. L. Westcott, A. J. Jircitano and K. A. Abboud, *Inorg. Chim. Acta*, 1995, **238**, 149.
4 C. Onindo, T. Yu. Sliva, T Kowalik-Jankowska, I. O. Fritsky, P. Buglyo, L. D. Pettit, H. Kozlowski and T. Kiss, *J. Chem. Soc., Dalton Trans.*, 1995, 3911.
5 B. Mernari, F. Abraham, M. Lagrenee, M. Dillon and P. Legoll, *J. Chem. Soc., Dalton Trans.*, 1993, 1707; F. Abraham, M. Lagrenee, S. Sueur, B. Mernari and C. Bremard, *J. Chem. Soc., Dalton Trans.*, 1991, 1443.
6 M. M. Aly, A. O. Baghlaf and N. S. Ganji, *Polyhedron*, 1985, **4**, 1301.
7 H. Okawa, T. Tokii, Y. Muto and S. Kida, *Bull. Chem. Soc. Jpn.*, 1973, **46**, 2464.
8 C. Krebs, M. Winter, T. Weyhermüller, E. Bill, K. Wieghardt and P. Chaudhuri, *J. Chem. Soc., Chem. Commun.*, 1995, 1913.
9 K. K. Nanda, A. W. Addison, N. Paterson, E. Sinn, L. K. Thompson and U. Sakaguchi, *Inorg. Chem.*, 1998, **37**, 1028.
10 E. V. Rybak-Akimova, D. H. Busch, P. K. Kahol, N. Pinto, N. W. Alcock and H. J. Clase, *Inorg. Chem.*, 1997, **36**, 510.
11 E. Buehler, *J. Org. Chem.*, 1967, **32**, 261; E. Buehler and G. B. Brown, *J. Org. Chem.*, 1967, **32**, 265; E. Falco and G. B. Brown, *J. Med. Chem.*, 1968, **11**, 142.
12 C. E. Pfluger and R. L. Harlow, *Acta Crystallogr.*, 1964, **17**, 1109.
13 A. Chakravorty, *Coord. Chem. Rev.*, 1974, **13**, 1 and refs. therein.
14 W. E. Hatfield, *Comments Inorg. Chem.*, 1981, **1**, 105.
15 A. P. Ginsberg, R. L. Martin, R. W. Brookes and R. C. Shewood, *Inorg. Chem.*, 1972, **11**, 2884.
16 See also, B. N. Figgis, *Introduction to Ligand Fields*, Wiley, New York, 1966; A. P. Ginsberg and M. E. Lines, *Inorg. Chem*, 1972, **11**, 2289; R. L. Carlin and J. N. McElearney, *Inorg. Chem.*, 1972, **11**, 2291; A. B. P. Lever, L. K. Thompson and W. M. Reiff, *Inorg. Chem.*, 1972, **11**, 2291.
17 R. L. Carlin, *Magnetochemistry*, Springer, Berlin, 1986.
18 S. Nakatsuka, K. Osaki and N. Uryu, *Inorg. Chem.*, 1982, **21**, 4332.
19 *Magnetostructural Correlations in Exchange Coupled Systems*, eds. D. Gatteschi, O. Kahn and R. D. Willett, Reidel, Dordrecht, 1984; O. Kahn, *Molecular Magnetism*, VCH, Weinheim, 1995.
20 V. H. Crawford, H. W. Richardson, J. R. Wasson, D. J. Hodgson and W. E. Hatfield, *Inorg. Chem.*, 1976, **15**, 2107.
21 L. K. Thompson, S. K. Mandal, S. S. Tandon, J. N. Bridson and M. K. Park, *Inorg. Chem.*, 1996, **35**, 3117.
22 K. K. Nanda, L. K. Thompson, J. N. Bridson and K. Nag, *J. Chem. Soc., Chem. Commun.*, 1994, 1337.
23 A. J. Blake, J. P. Danks, A. Harrison, S. Parsons, P. Schooler, G. Whittaker and M. Schröder, *J. Chem. Soc., Dalton Trans.*, 1998, 2335; A. J. Blake, J. P. Danks, I. A. Fallis, A. Harrison, W.-S. Li, S. Parsons, S. A. Ross, G. Whittaker and M. Schröder, *J. Chem. Soc., Dalton Trans.*, 1998, 3969.
24 S. L. Lambert and D. N. Hendrickson, *Inorg. Chem.*, 1979, **18**, 2683.
25 R. K. Nesbet, *Ann. Phys.*, 1958, **4**, 87.
26 C. J. O'Connor, *Prog. Inorg. Chem.*, 1982, **29**, 203.
27 F. Ullman and K. Brittner, *Berichte*, 1909, **42**, 2539.
28 S. K. Mandal and K. Nag, *J. Chem. Soc., Dalton Trans.*, 1983, 2429.
29 G. M. Sheldrick, SHELXS 86, program for crystal structure solution, *Acta Crystallogr., Sect. A*, 1990, **46**, 467.
30 G. M. Sheldrick, SHELXL 93, program for crystal structure refinement, University of Göttingen, 1993.
31 J. Cosier and A. M. Glazer, *J. Appl. Crystallogr.*, 1986, **19**, 105.
32 G. M. Sheldrick, SHELX 76, program for crystal structure refinement, University of Cambridge, 1976.

*Paper 8/07031H*